Synthesis, characterization and study of photocatalytic activity of nanocomposites of oxides and sulfides of Ni(II) and Ni(III)

H. R. Pouretedal[1]*, F. Momenzadeh[2]

[1] Faculty of Applied Chemistry, Malek-ashtar University of Technology, Shahin-Shahr, Iran,

[2] Department of Chemistry, Islamic Azad University, Shahreza Branch, Shahreza, Iran

Nanoparticles of NiO, NiS, Ni_2O_3, Ni_2S_3, $NiO_{0.5}S_{0.5}$ and $Ni_2O_{1.5}S_{1.5}$ were synthesized by a controlled precipitation method. The prepared nanoparticles were calcined at temperature 700 ℃. The X-ray diffraction patterns of the nanoparticles showed cubic structure for NiO, Ni_2O_3, Ni_2S_3, $NiO_{0.5}S_{0.5}$ and $Ni_2O_{1.5}S_{1.5}$, while the nanosized NiS displayed cubic and hexagonal structure. The absorption peaks at wavenumbers of 600-400 cm^{-1} in the FT-IR spectra showed the existence of S-Ni and S-Ni-S vibrations. A red shift of 30 nm was observed in the DRS UV-Vis spectra of $NiO_{0.5}S_{0.5}$ and $Ni_2O_{1.5}S_{1.5}$ nanocomposites with respect to the nanoparticles of oxide and sulfide of Ni (II) and Ni(III). The band-gap energies were 5.79, 5.71, 5.64, 5.51, 4.96 and 4.86 eV for Ni_2S_3, Ni_2O_3, NiO, NiS, $NiO_{0.5}S_{0.5}$ and $Ni_2O_{1.5}S_{1.5}$, respectively. The TEM image showed that the size of the $Ni_2O_{1.5}S_{1.5}$ nanocomposite was less than 70 nm. The existence of Ni, S and O atoms in the structure of $Ni_2O_{1.5}S_{1.5}$ nanocomposite was proved by energy dispersive X-ray analysis. The photocatalytic activity of the prepared nanoparticles was studied in the photodegradation reaction of methyl blue dye. The trend of the photocatalytic activity of the prepared nanoparticles in photodegradation of methyl blue was: $Ni_2O_{1.5}S_{1.5} > NiO_{0.5}S_{0.5} > NiS > NiO > Ni_2O_3 > Ni_2S_3$. The pH of the point of zero charge of the nanocomposites was ~6.0. The optimized conditions of the photodegradation process were: pH 7, 0.5 g L^{-1} of photocatalyst, 20 mg L^{-1} of dye and irradiation time of 60 min.

Keywords: Nanocomposite, nanoparticle, photocatalyst, methyl blue, nickel.

INTRODUCTION

High-efficiency photocatalysts have been actively sought due to their potential applications in the decomposition of toxic and hazardous materials [1,2], in water splitting for hydrogen energy production [3,4] and in photoelectrochemical or solar cell devices [5,6]. There have been various kinds of efforts to develop more efficient versions of photocatalysts than the well-known TiO_2 [7].

Intense research activity is seen in recent years in advancing the synthesis and functionalization of various sizes and shapes of semiconductors as photocatalysts. The goal of these activities is to improve the performance and utilization of nanophotocatalysts in order to enhance the efficiency of advanced oxidation techniques (AOTs) [8]. The photocatalytic activity is dependent on the size and shape of the photocatalyst particles. Maximizing the efficiency of photoinduced charge separation in semiconductor systems remains a major challenge to the scientific community [9]. Obtaining insight into charge transfer processes is important to improve the photoconversion efficiencies in semiconductor-based nanoassemblies. Extending the photoresponse of the particles is a common goal and improving efficiency by using various combinations of particle materials is often attempted. Quantization and its effects on charge transfer, the processes that are induced by charge separation at the particle surface are the focus of many of the current advances in the field and dual use of these materials, as well as combination of AOTs is often explored [10,11].

In recent years, research on the coupling of semiconductor photocatalysts as nanocomposite alloys has taken place for increasing the efficiency of AOTs. The coupling of photocatalyst nanoparticles is due to interfacial charge transfer between two different semiconductors with disparately favorable band edge energy levels [12,14].

Although charge transfer to adsorbate species is the desired behavior of electron-hole pairs (EHPs), the vast majorities recombine, creating a loss in photocatalytic efficiency often greater than 90%. This recombination process between the photoexcited electron and the hole can occur either in the bulk of the semiconductor particle or on its surface with a byproduct of heat release [15]. The EHP recombination process itself results when the electron-hole recombination time is shorter than the time needed by the carrier to diffuse to the surface.

The use of nanocomposite alloys as photocatalysts can extend the electron-hole recombination time. Thus, an increase in reactivity of electron/hole (e/h$^+$) pairs is observed with reduction of the rate of electron-hole recombination [16].

The most common semiconducting metal oxide is TiO_2. However, other semiconducting metal oxides and metal sulfides such as NiO and NiS appear to be especially efficient as catalysts for wastewater pollution abatement. NiO is a p-type semiconductor characterized by a wide band gap between 3.1-3.5 eV that makes it suitable for photocatalytic processes [17,18].

NiS (a p-type semiconductor) is showing metal-insulator transition by doping or as a function of temperature and pressure. NiS semiconductor shows antiferromagnetic and paramagnetic properties in low and high temperature phases, respectively [19,20]. NiS films have been used as catalysts and coatings in photovoltaic cells. Catalysts have broad application in oil industry, for the separation of sulphur and nitrogen that often coexist with hydro-compounds from insulators. NiS is used as a holder in hydro-process catalysts [21,22].

The goal of this research is the synthesis of nanocomposites of oxides and sulfides of Ni(II) and Ni(III) as $NiO_{0.5}S_{0.5}$ and $Ni_2O_{1.5}S_{1.5}$. The photocatalytic activity of the prepared nanoconposites is studied in the photodegradation process of methyl blue dye and compared with the reactivity of NiO, NiS, Ni_2O_3 and Ni_2S_3 nanoparticles. The photocatalytic activity of the nanocomposites is discussed on the basis of the results of nanoparticles characterization.

EXPERIMENTAL

Preparation of nanocomposites

Nanosized powders of NiO, NiS, Ni_2O_3, Ni_2S_3, $NiO_{0.5}S_{0.5}$ and $Ni_2O_{1.5}S_{1.5}$ were prepared by precipitation and co-precipitation methods [23,24]. $Ni(NO_3)_2 \cdot 6H_2O$ was used as the precursor and ammonia (1:1) and $Na_2S \cdot 9H_2O$ were used as precipitants. The $Ni(OH)_2$ precipitate was formed with addition of ammonia solution to Ni^{2+} solution (50 ml 0.05 mol/L) at room temperature under vigorous stirring. The pH of the sample was maintained at pH=5.0. The sulfide solution (0.05 mol/L) was added drop-wise so that the Ni(II) ions were completely transformed to the precipitate NiS. The oxidizing agent $KClO_3$ was used to oxidize Ni(II) to Ni(III) for the preparation of Ni_2O_3 and Ni_2S_3 powders. Stoichiometric amounts of ammonia and/or Na_2S were added to a solution containing 0.05 mol/L of Ni^{2+} and 0.1 mol/L of $KClO_3$. Then, the precipitates of $Ni(OH)_3$ and Ni_2S_3 were used to prepare nanoparticles of Ni_2O_3 and Ni_2S_3, respectively. For preparation of $NiO_{0.5}S_{0.5}$ nanocomposite, stoichiometric amount of sulfide solution was added to Ni(II) solution so that half of the nickel ions was converted to NiS and then the pH of the samples was brought to 5 with addition of ammonia solution for conversion of the other half of Ni^{2+} ions to $Ni(OH)_2$ precipitate. The nanocomposite $Ni_2O_{1.5}S_{1.5}$ was prepared similarly to the $NiO_{0.5}S_{0.5}$ nanocomposite using $KClO_3$ to oxidize Ni(II) to Ni(III) ions.

The formed precipitates were filtered and washed with deionized water and ethanol. The wet powders were dried at about 100 °C and then calcined at a temperature of 700 °C in air for 4 h.

Characterization of the nanoparticles

The XRD patterns of the nanoparticles were obtained on a diffractometer Bruker D8 ADVANCE, Germany with Cu anode (λ=1.5406 Å of Cu Kα) and Ni filter. A JEOL JEM-1200EXII transmission electron microscope (TEM) operating at 120 kV was used for estimation of nanoparticles size. The supporting grids were formvar-covered, carbon-coated 200-mesh copper grids. A Philips XL30 scanning electron microscope was used to observe the composition of the nanocomposites. The absorbance spectra of the prepared nanosized materials were recorded by a UV-Vis spectrophotometer Carry-100. Nicolet Impact 400D FT-IR spectrophotometer was used to record the IR-spectra of the prepared photocatalysts in the range 4000-400 cm^{-1}.

Photocatalytic activity

The photocatalytic activity of the prepared nanoparticles and nanocomposites was studied in the photodegradation reaction of methyl blue dye. The samples were irradiated in a photoreactor containing a 36 W mercury low-pressure lamp. A light path of 5.0 cm was used in the photoreactor cell. The photoreactor was filled with 100 ml of 20 mg/L of methyl blue and 0.1-3.0 g/L of the photocatalyst at a pH of 2-9. The pH of the samples was adjusted by sodium hydroxide and hydrochloric acid solutions of concentration 0.1 mol/L. A water-cooled jacket was applied outside the photoreactor to maintain the temperature at 30 °C. All reactants in the degradation reaction were stirred in the photoreactor cell by a magnetic stirrer for 30-180 min. A time of 30 min in dark was applied to set the adsorption/desorption

equilibrium of methyl blue on the surface of the heterogeneous catalysts.

A UV-Vis spectrophotometer Carry-100 was used to measure the absorbance of the samples before and after definite times of irradiation. The decoloration efficiency (%D) was obtained as: %D = 100 × [(Co-Ct)/Co]. The Co and Ct were the initial and the final concentration at a time, respectively. A centrifuge was used to separate suspended particles before absorbance measurement.

The pH of samples played an important role in the decoloration of dye. The pH of point of zero charge (pH of PZC) of nanocomposites was determined as follows. The initial pH values of several suspensions containing 1.0 g/L of the nanoparticles and 1.0 mol/L of NaCl were adjusted to 2-9 with addition of HCl and NaOH solutions. After 24 h, the final pH values of the suspensions were measured again. The pH of PZC was obtained from the intersection of the curve of initial pHs *versus* final pHs with the diagonal of square [25].

RESULTS AND DISCUSSION

Characterization of nanoparticles

The XRD patterns of the prepared nanoparticles of NiO, NiS, Ni_2O_3, Ni_2S_3, $NiO_{0.5}S_{0.5}$ and $Ni_2O_{1.5}S_{1.5}$ are shown in Fig. 1.
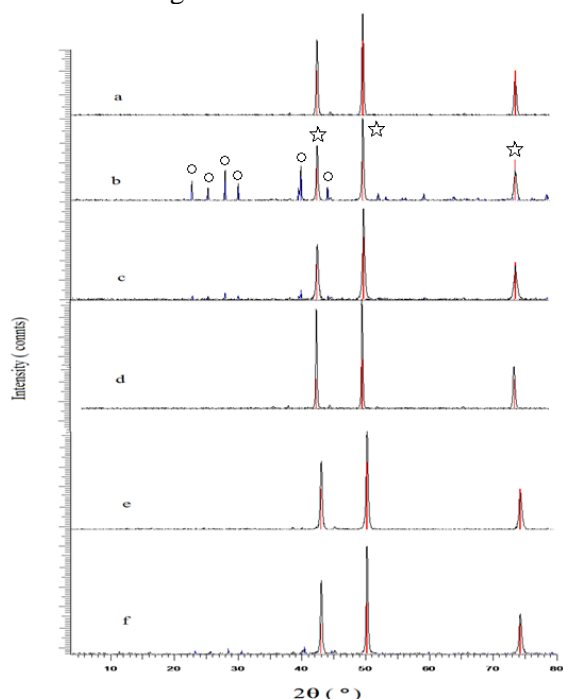

Fig. 1. XRD patterns of nanoparticles of (a) NiO, (b) NiS, (c) $NiO_{0.5}S_{0.5}$, (d) Ni_2O_3, (e) Ni_2S_3, and (f) $Ni_2O_{1.5}S_{1.5}$ calcined at 700 ºC. The signs of star and circle show the peaks of cubic and hexagonal structure, respectively.

The XRD patterns are shown below for comparison. The scale on the vertical axis is the same for all XRD patterns. The nanosized powders were calcined at a temperature of 700 ºC. As seen, a cubic structure with diffraction peaks at 2θ of 43, 50 and 74º was observed for NiO, Ni_2O_3 and Ni_2S_3 nanoparticles [26-29]. For nanosized NiS the diffraction peaks at 2θ of 22, 24, 27, 29, 39 and 43º were related to the hexagonal structure and diffraction peaks at 2θ of 43, 50 and 74º were related to the cubic structure [21,22,26,27]. The nanocomposites of Ni_2S_3 $NiO_{0.5}S_{0.5}$ and $Ni_2O_{1.5}S_{1.5}$, as well as the other oxides and sulfides of Ni(II) and Ni(III) showed a cubic structure with diffraction peaks at 2θ of 43, 50 and 74º.

The crystallite size D of the nanoparticles was estimated by the Schererr's formula (D = kλ/βcosθ), where k is a constant = 0.94, λ is the X-ray wavelength, θ is the Bragg angle of the peak under consideration and β is the full width at half maximum (FWHM) of the diffraction peak [28,29]. The size of the prepared nanoparticles thus obtained was < 25 nm.

The FT-IR spectra of the nanocomposites of $NiO_{0.5}S_{0.5}$ and $Ni_2O_{1.5}S_{1.5}$ calcined at temperature of 700 ºC are shown in Fig. 2.
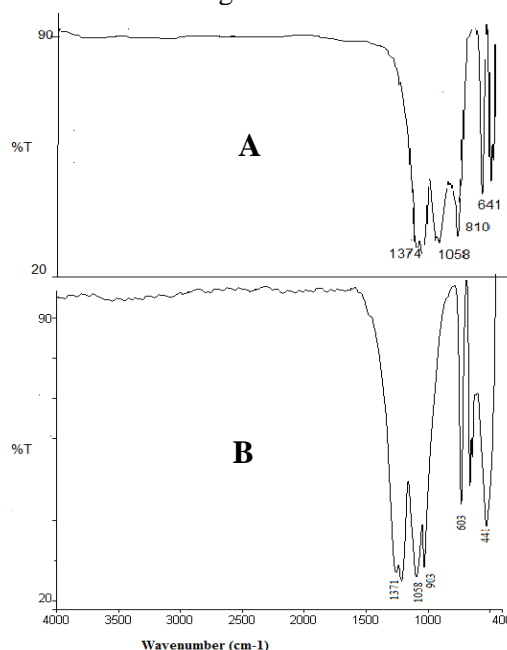

Fig. 2. FT-IR spectra of nanocomposites of $NiO_{0.5}S_{0.5}$ (A) and $Ni_2O_{1.5}S_{1.5}$ (B).

The bands in the range of 1370-800 cm^{-1} can be attributed to vibrations of stretching and bending of the nitrogen-oxygen, sulfur-oxygen and nitrogen-sulfur bonds. The peaks at 441 and 603 cm^{-1} were

due to the metal-nonmetal (Ni-S, Ni-O, S-Ni-S and O-Ni-O) stretch [30,31].

It is well known that the photocatalytic activity of a photocatalyst is dependent on the band-gap energy. The UV-Vis absorption bands can be used to determine band-gap energies of semiconductor materials. The DRS UV-Vis spectra of the prepared nanoparticles are shown in Fig. 3.
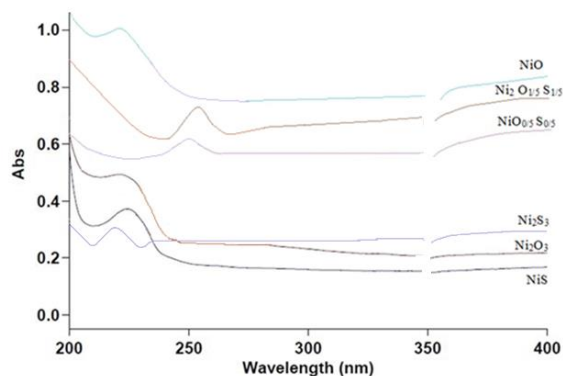

Fig. 3. UV-Vis spectra of the prepared nanoparticles calcined at 700 °C.

The absorption bands show maximum absorption at wavelengths (λ_{max}) of 214, 217, 220, 225, 250 and 255 nm for Ni_2S_3, Ni_2O_3, NiO, NiS, $NiO_{0.5}S_{0.5}$ and $Ni_2O_{1.5}S_{1.5}$, respectively. The band-gap was calculated using the Planck's equation (Band-gap, eV = 1240/ λ_{max}, nm) [32]. Band-gap energies of 5.79, 5.71, 5.64, 5.51, 4.96 and 4.86 eV were obtained for Ni_2S_3, Ni_2O_3, NiO, NiS, $NiO_{0.5}S_{0.5}$ and $Ni_2O_{1.5}S_{1.5}$, respectively. Therefore, the obtained results showed that the nanocomposites of oxides and sulfides of Ni(II) and Ni(III) have a lower band-gap energy in comparison with the Ni_2S_3, Ni_2O_3, NiO and NiS nanoparticles. Also, the absorption spectrum of Ni_2S_3, Ni_2O_3, NiO and NiS nanoparticles shows an obvious blue shift compared with that of bulk oxides and sulfides of nickel (~2.1 - ~3.9 eV) [26-29,33]. The increase in the surface area of the nanoparticles *versus* bulk materials is an important factor for photocatalysts. The band-gap energy increases with decreasing the size of the prepared particles, so that the increasing in band-gap can be due to a decrease in photocatalytic activity [33,34]. However, the synthesis of nanocomposites can be a solution for excessive perversion of band-gap energy. So, a red shift is seen at the λmax of the nanocomposites of $NiO_{0.5}S_{0.5}$ and $Ni_2O_{1.5}S_{1.5}$ compared with NiO, NiS, Ni_2S_3 and Ni_2O_3, respectively.

The size of the nanocomposite particles of $Ni_2O_{1.5}S_{1.5}$ was further examined by transmission electron microscopy (TEM). The TEM image of the synthesized $Ni_2O_{1.5}S_{1.5}$ is shown in Fig. 4.

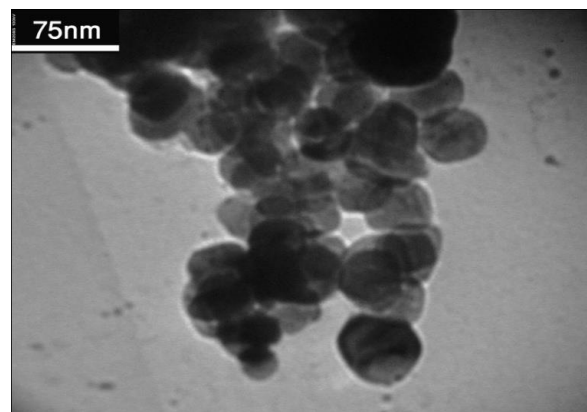**Fig. 4.** TEM image of the nanocomposite of $Ni_2O_{1.5}S_{1.5}$ calcined at 700 °C.

The micrograph shows that the nanoparticles are uniformly distributed and are almost spherical in shape. The size of the obtained particles is less than 75 nm.

Energy dispersive spectroscopy (EDS) can be used for qualitative analysis of elements in a composite. Figure 5 shows the EDS spectrum of $Ni_2O_{1.5}S_{1.5}$ nanocomposite that confirms the presence of nickel, oxygen and sulfur in the obtained composite [31].

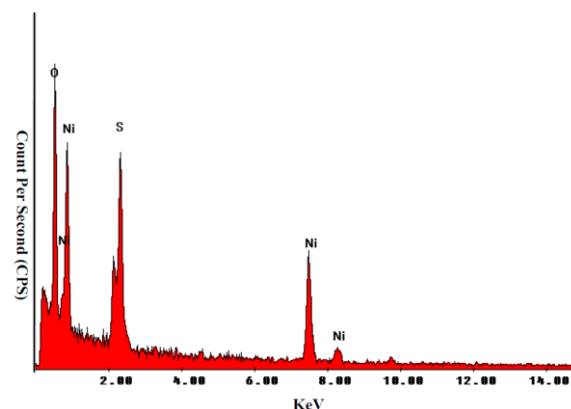**Fig. 5.** Energy-dispersive X-ray analysis (EDAX) of the nanocomposite of $Ni_2O_{1.5}S_{1.5}$ calcined at 700 °C.

Photocatalytic activity of nanocomposites

The photocatalytic activity of the prepared nanoparticles was studied in methyl blue photodegradation. The optimized conditions were found by using one-factor-at-a-time method. pH of samples, dose of photocatalysts, initial concentration of dye and irradiation time were the investigated factors.

At first, the pH of the samples was optimized because the surface charge of semiconductors in aqueous samples and the charge of dye molecules are pH-dependent. It is well known that the surface charge of semiconductors is also dependent on the pH of point of zero charge (pH_{PZC}) [35,36]. The

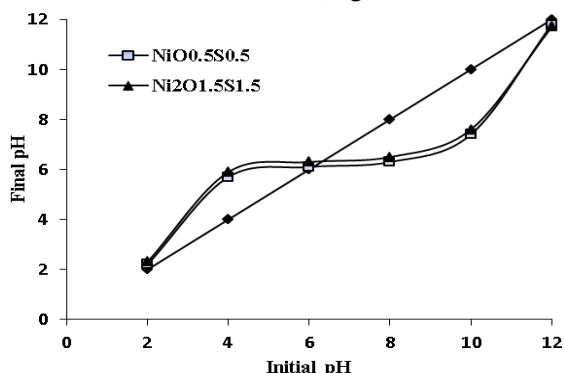pH_{PZC} of the nanocomposites of $NiO_{0.5}S_{0.5}$ and $Ni_2O_{1.5}S_{1.5}$ has a value of ~6 (Fig. 6).

Fig. 6. The pH_{PZC} of nanocomposites of $NiO_{0.5}S_{0.5}$ and $Ni_2O_{1.5}S_{1.5}$.

As a result, the pH_{PZC} of Ni_2S_3, Ni_2O_3, NiO and NiS nanoparticles is also ~6. Therefore, the surface charge of semiconductors is positive at pHs < 6 and negative at pHs > 6. The effect of pH of samples on the reactivity of photocatalysts is indicated in Fig. 7.
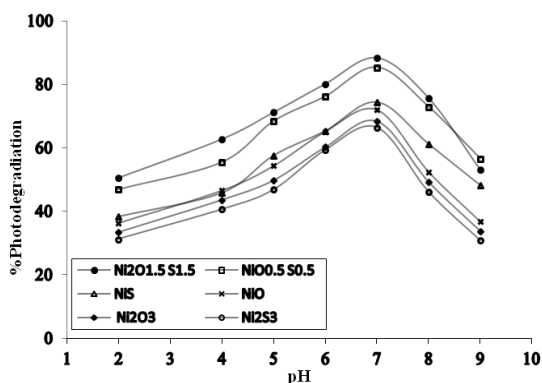

Fig. 7. Effect of pH on the photodegradation efficiency of methyl blue using 0.25 g/L of photocatalyst, 20 mg/L of dye and irradiation time of 60 min.

The highest reactivity was obtained at pH 7. Based on the pH_{PZC} of nanocomposites, the surface of semiconductors is neutral at pH 7. Thus, the pollutant molecules with neutral and/or negative charges are adsorbed on the surface of the catalysts at pH 7. The photodegradation yields decrease at alkaline pHs because there is a repulsion force between the charge of dye molecules and the surface charge of photocatalyst nanoparticles at pH > 7.

Fig. 8 shows that the photocatalytic efficiency of the prepared nanoparticles increases with increasing the dose of photocatalysts up to 0.5 g/L and then decreases. The turbidity of the suspension of heterogeneous catalysts at high amounts is due to a decrease in radiation penetration [37].
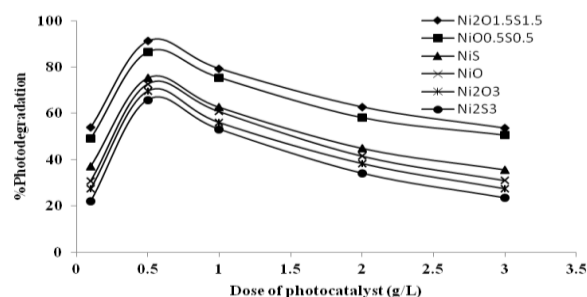

Fig. 8. Effect of photocatalyst dose on the photodegradation efficiency of methyl blue at pH 7, 20 mg/L of dye and irradiation time of 60 min.

The photocatalytic activity was also studied by determining the kinetics of methyl blue photodegradation reaction at initial concentration of 20 mg/L of dye, pH of 7 and 0.5 g/L of photocatalyst. The pseudo-first-order rate constants, k_{obs} (min^{-1}), were obtained using Langmuir–Hinshelwood kinetic expression ($\ln(C_o/C_t)=k_{obs}t$) [38]. The obtained curves are shown in Fig. 9 and the k_{obs} values are collected in Table 1.
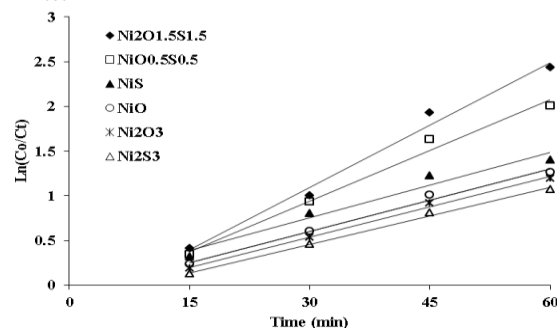

Fig. 9. The variations of $\ln(C_o/C_t)$ *versus* time for methyl blue photodegradation reaction in presence of different photocatalysts.

The data of Table 1 show that the order of photocatalytic activity of the nanoparticles is: $Ni_2O_{1.5}S_{1.5}$ > $NiO_{0.5}S_{0.5}$ > NiS > NiO > Ni_2O_3 > Ni_2S_3.

As mentioned, the band-gap energies of Ni_2S_3, Ni_2O_3, NiO, NiS, $NiO_{0.5}S_{0.5}$ and $Ni_2O_{1.5}S_{1.5}$ are: 5.79, 5.71, 5.64, 5.51, 4.96 and 4.86 eV, respectively. Thus, the proposed nanocomposites with lower band-gap energy show higher photocatalytic activity. The new nanocomposites, as well as the nanoparticles of oxides and sulfides of Ni(II) and Ni(III) have higher band-gap energy than their bulk materials. However, the increase in band-gap can be an advantage for a photocatalyst.

Recombination of electrons and holes in a semiconductor is a restricting factor for photocatalytic activity. The lifetime of electrons and holes in conductance and capacitance bands, respectively, increases with addition of band-gap

Table 1. The $k_{obs} \pm S_D$ values of methyl blue photodegradation reaction catalyzed by the prepared photocatalysts, S_D is standard deviation related to n=3.

Photocatalyst	$Ni_2O_{1.5}S_{1.5}$	$NiO_{0.5}S_{0.5}$	NiS	NiO	Ni_2O_3	Ni_2S_3
k_{obs} (min^{-1})	$46.6 \pm 1.2 \times 10^{-3}$	$37.8 \pm 1.0 \times 10^{-3}$	$24.4 \pm 1.1 \times 10^{-3}$	$23.3 \pm 0.9 \times 10^{-3}$	$22.6 \pm 1.0 \times 10^{-3}$	$21.3 \pm 0.7 \times 10^{-3}$

energy. At these conditions, the concentration of active radicals such as $^{\bullet}OH$ radicals increases, thus increasing of the kinetics of degradation reaction is expected. On the other hand, available sites on a heterogeneous catalyst increase with decreasing size of particles. Thus, higher rate for photodegradation of a pollutant is achieved by using the new nanocomposites [39,40].

CONCLUSIONS

A simple precipitation method can be used to prepare new nanocomposites of $NiO_{0.5}S_{0.5}$ and $Ni_2O_{1.5}S_{1.5}$. The proposed nanosized composites of nickel oxide and sulfide have a narrower band-gap in comparison with nickel oxide and nickel sulfide. The new nanocomposites exhibit higher photocatalytic activity.

REFERENCES

1. L.L. Garza-Tovar, L.M. Torres-Martinez, D. B. Rodriguez, R. Gomez, G. del Angel, *J. Mol. Catal*., **A 247**, 283 (2006).
2. V.N. Blaskov, I.D. Stambolova, S.V. Vassilev, *Bulgarian Chem. Commun*. 45, 263 (2013).
   3. P. Dhanasekaran, N.M. Gupta, *Intern. J. Hydrogen Energy* , **37**, 4897 (2012).
3. H. Hagiwara, M. Nagatomo, C. Seto, S. Ida, T. Ishihara, *J. Photochem. Photobiol*., **A 272**, 41 (2013).
4. N.G. Dhere, A.H. Jahagirdar, *Thin Solid Films* , **480–481**, 462 (2005).
5. R. Afeesh, N.A.M. Barakat, S.S. Al-Deyab, A. Yousef, H.Y. Kim, *Colloids Surfaces,* **A 409**, 21 (2012).
6. A.L. Linsebigler, G. Lu, J.T. Yates, *Chem. Rev*., **95**, 735 (1995).
7. G. Gyawali, R. Adhikari, B. Joshi, T.H. Kim, V. Rodríguez-González, S.W. Lee, *J. Hazard. Mater*., **263**, 45 (2013).
8. L. Cheng, Y. Kang, *J. Alloy Compd*. 585, 85 (2014).
9. R. Adhikari, G. Gyawali, S. H. Cho, R. Narro-García, T. Sekino, S.W. Lee, *J. Solid State Chem*., **209**, 74 (2014).
10. G. Wu, S. S. Thind, J. Wen, K. Yan, A. Chen, *Appl. Catal*., **B 142–143**, 590 (2013).
11. K. Sridharan, E. Jang, T. J. Park, *Appl. Catal*., **B 142–143**, 718 (2013).
12. Y. Yu, G. Chen, G. Wang, Z. Lv, *Intern. J. Hydrogen Energy,* **38**, 1278 (2013).
13. X. Fu, W. Tang, L. Ji, S. Chen, *Chem. Eng. J*.,**180**, 170 (2012).
14. X. Pan, Y.-J. Xu, *Appl. Catal., A 459*, 34 (2013).
15. J. Chen, G. Li, Y. Huang, H. Zhang, H. Zhao, T. An, *Appl. Catal., B 123–124*, 69 (2012).
16. L. Li, K.S. Hui, K.N. Hui, H.W. Parka, D.H. Hwang, S. Cho, S.K. Lee, P.K. Song, Y.R. Cho, H. Lee, Y.G. Son, W. Zhou, *Mater. Lett*., **68**, 283 (2012).
17. A. K. Srivastava, S. Thota, J. Kumar, *J. Nanosci. Nanotechnol*., **8**, 4111 (2008).
18. M. Banerjee, L. Chongad, A. Sharma, *Res. J. Recent Sci.,* **2**, 326 (2013).
19. A. Sharma, S. Rastogi, M. Sindal, *Int. J. Chem. Sci*., **9**, 1569 (2011).
20. F. Atay, S. Kose, V. Bilgin, I. Akyuz, Electrical, *Turk. J. Phys*., **27**, 285 (2003).
21. M. Barman, S. Paul, A. Sarkar, *Adv. Appl. Sci. Res*., **4**, 343 (2013).
22. H. R. Pouretedal, M. Tavakkoli, *Desalination Water Treat*. 51, 4744 (2013).
23. H.R. Pouretedal, Z. Tofangsazi, M.H. Keshavarz, *J. Alloy Compd*., **513**, 359 (2012).
24. H. R. Pouretedal, M. Kiyani, *J. Iran. Chem. Soc.,* DOI 10.1007/s13738-013-0297-2.
25. H. Zhou, B. Lv, D. Wu, Y. Sun, *Particuology,* **10**, 783 (2012).
26. N. Chen, W. Zhang, W. Yu, Y. Qian, *Mater. Lett*., **55**, 230 (2002).
27. A.G. Al-Sehemi, A.S. Al-Shihri, A. Kalam, G. Du, T. Ahmad, *J. Mole. Structure,* **1058**, 56 (2014).
28. M.A. Behnajady, S. Bimeghdar, *Chem. Eng*. J. **239**, 105 (2014).
29. Q. Li, L.-S. Wang, B.-Y. Hu, C. Yang, L. Zhou, L. Zhang, *Mater. Lett*. , **61**, 1615 (2007).
30. M. Salavati-Niasari, F. Davar, H. Emadi, *Chalcogenide Lett*. , **7**, 647 (2010).
31. D. Rezaei Ochbelagh, N. Morsali Golboos, Sh. Sohrabnezhad, *Radiation Phys. Chem*., **87**, 1 (2013).
32. N. Li, B. Zhou, P. Guo, J. Zhou, D. Jing, *Int. J. Hydrogen Energy,* **38**, 11268 (2013).
33. A. Nezamzadeh Ejhieh, M. Khorsandi, *J. Hazard. Mater*. , **176**, 629 (2010).
34. H. R. Pouretedal, A. Shafeie, M. H. Keshavarz, *J. Korean Chem. Soc*., **56**, 484 (2012).
35. G. Zhang, W. Zhang, D. Minakata, Y. Chen, J. Crittenden, P. Wang, *Int. J. Hydrogen Energy,* **38**, 11727 (2013).
36. H.R. Pouretedal, S. Basati, *Iran. J. Catal*., **2**, 50 (2012).
37. K. Ullah, S. Ye, L. Zhu, Z.-D. Meng, S. Sarkar, W.-C. Oh, *Mater. Sci. Eng*., **B 180**, 20 (2014).
38. H.R. Pouretedal, H. Motamedi, A. Amiri, *Desalination Water Treat.,* **44**, 92 (2012).
39. N. Kaneva1, A. Ponomareva, L. Krasteva, D. Dimitrov, A. Bojinova, K. Papazova, G. Suchaneck, V. Moshnikov, *Bulgarian Chem. Commun*., **45**, 635 (2013).

СИНТЕЗА, ОХАРАКТЕРИЗИРАНЕ И ИЗСЛЕДВАНЕ НА ФОТОКАТАЛИТИЧНАТА АКТИВНОСТ НА НАНОКОМПОЗИТИ ОТ ОКИСИ И СУЛФИДИ НА Ni(II) И Ni(III)

Х.Р. Пуретедал [1*], Ф. Момензаде[2]

[1] *Факултет по приложна химия, Технологичен университет Малек-ащар, Шахин Шахр, Иран*
[2] *Департамент по химия, Ислямски университет "Азад", Клон Шахреза, Шахреза, Иран*

(Резюме)

Синтезирани са наночастици от NiO, NiS, Ni_2O_3, Ni_2S_3, $NiO_{0.5}S_{0.5}$ и $Ni_2O_{1.5}S_{1.5}$ по метода на контролираното утаяване. Приготвените наночастици са калцинирани при 700 ºC. Рентгено-дифракционните изследвания показват кубична структура за NiO, Ni_2O_3, Ni_2S_3, $NiO_{0.5}S_{0.5}$ и $Ni_2O_{1.5}S_{1.5}$, а при наноразмерните частици от NiS се наблюдават както кубична, така и хексагонална структура. Абсорбционните пикове в FT-IR спектрите при вълнови числа 600-400 cm^{-1} показват наличието на вибрации на връзките S-Ni и S-Ni-S. Наблюдава се червено отместване от 30 nm в DRS UV-Vis – спектрите на нанокомпозитите от $NiO_{0.5}S_{0.5}$ и $Ni_2O_{1.5}S_{1.5}$ спрямо наночастиците на оксидите и сулфидите на Ni (II) и Ni(III). Енергийни ями 5.79, 5.71, 5.64, 5.51, 4.96 and 4.86 eV са получени съответно Ni_2S_3, Ni_2O_3, NiO, NiS, $NiO_{0.5}S_{0.5}$ и $Ni_2O_{1.5}S_{1.5}$. TEM-микроскопски снимки показват, че размерите на нанокомпозитите от $Ni_2O_{1.5}S_{1.5}$ са под 70 nm. Съществуването на атоми от Ni, S и О в структурата на нанокомпозитите от $Ni_2O_{1.5}S_{1.5}$ е доказано чрез дисперсионен рентгенов анализ. Фотокаталитичната активност на приготвените наночастици е изследвана върху фото-разпадането на метиленово синьо. Фотокаталитичната активност на изследваните наночастици за тази реакция е както следва: $Ni_2O_{1.5}S_{1.5}$ > $NiO_{0.5}S_{0.5}$ > NiS > NiO > Ni_2O_3 > Ni_2S_3. Стойността на pH в точката на нулев товар е ~6.0. Оптимизираните условия за този процес на фотодеградация са: pH 7, 0.5 g L^{-1} фотокатализатор, 20 mg L^{-1} багрило и време на облъчване 60 мин.